

## ***FUSE* Detection of Galactic O VI Emission in the Halo above the Perseus Arm**

Birgit Otte, W. Van Dyke Dixon, Ravi Sankrit

*Department of Physics and Astronomy, The Johns Hopkins University, 3400 North Charles Street, Baltimore, MD 21218*

otte@pha.jhu.edu, wvd@pha.jhu.edu, ravi@pha.jhu.edu

### **ABSTRACT**

Background observations obtained with the *Far Ultraviolet Spectroscopic Explorer (FUSE)* toward  $l = 95^{\circ}4$ ,  $b = 36^{\circ}1$  show O VI  $\lambda\lambda 1032, 1038$  in emission. This sight line probes a region of stronger-than-average soft X-ray emission in the direction of high-velocity cloud Complex C above a part of the disk where H $\alpha$  filaments rise into the halo. The O VI intensities,  $1600 \pm 300$  photons  $\text{s}^{-1} \text{cm}^{-2} \text{sr}^{-1}$  (1032 Å) and  $800 \pm 300$  photons  $\text{s}^{-1} \text{cm}^{-2} \text{sr}^{-1}$  (1038 Å), are the lowest detected in emission in the Milky Way to date. A second sight line nearby ( $l = 99^{\circ}3$ ,  $b = 43^{\circ}3$ ) also shows O VI  $\lambda 1032$  emission, but with too low a signal-to-noise ratio to obtain reliable measurements. The measured intensities, velocities, and FWHMs of the O VI doublet and the C II\* line at 1037 Å are consistent with a model in which the observed emission is produced in the Galactic halo by hot gas ejected by supernovae in the Perseus arm. An association of the observed gas with Complex C appears unlikely.

*Subject headings:* ISM: general — ISM: kinematics and dynamics — ISM: structure — Galaxy: halo — Galaxy: kinematics and dynamics — Galaxy: structure

### **1. INTRODUCTION**

The interstellar medium (ISM) consists of several phases. The hottest phase reaches temperatures of a few million degrees and is observed in X-ray emission. Gas at slightly cooler temperatures ( $\sim 3 \times 10^5$  K) is best traced by O VI, which has a strong resonance doublet at 1032/1038 Å. The O VI ion is generally assumed to trace collisionally-ionized gas,

because photoionization by hot stars cannot easily create such high ionization states in the diffuse ISM (e.g., Martin & Bowyer 1990). Possible scenarios for the production of O VI include the cooling of gas originally heated by supernova shocks and turbulent mixing of hot and cold gas at the surfaces of infalling high-velocity clouds (HVCs) as they pass through the Galactic corona.

To date, Galactic O VI  $\lambda 1032$  has been observed in emission along six sight lines with the *Far Ultraviolet Spectroscopic Explorer (FUSE)* (Dixon et al. 2001; Shelton et al. 2001; Shelton 2002a; Welsh et al. 2002). The location of the O VI emitting gas along these sight lines is generally unknown. Welsh et al. (2002) note the narrow range of the observed intensities and suggest that the O VI emission originates in the boundary of the Local Bubble. Absorption-line measurements along about 100 sight lines (Savage et al. 2002) reveal only a poor correlation of O VI with other tracers of the ISM, such as neutral and ionized hydrogen or soft X-ray (SXR) emission. Savage et al. (2002) conclude that the observed O VI absorption is best explained by a patchy, absorbing disk with a scale height of about 2.3 kpc. This thick disk corotates with the Galactic plane and shows signs of outflow along about 20% of the observed sight lines.

We have observed O VI emission along two sight lines, only one of which allows reliable measurements using line profile fitting. We compare the physical parameters of the O VI emission lines along this sight line with gaseous features observed at other wavelengths representing different phases of the ISM to determine the location of the O VI emitting gas and to investigate possible processes leading to the observed O VI emission.

## 2. OBSERVATIONS AND DATA REDUCTION

Our data sets (program IDs S4054801 and S4056101, hereafter SL5 and SL6, respectively) were obtained with *FUSE* as background observations recorded in time-tag mode on 2002 January 19–22. Our data are the first observations taken after the recovery of the satellite from a reaction wheel failure in December 2001 (Ake et al. 2002). We used the data obtained through the low-resolution (LWRS) aperture ( $30'' \times 30''$ ) on detector segment LiF1A (see Moos et al. (2000) and Sahnou et al. (2000) for a complete description of *FUSE* and its on-orbit performance). The total exposure time of the 55 exposures of SL5 was 217 ksec, with 95 ksec recorded during orbital night. The eight exposures of SL6 yielded a total exposure time of 32 ksec, with 13 ksec during orbital night. During these observations, the satellite was pointed near the orbital pole (see Table 1 for observational data).

The data were processed using the CALFUSE pipeline version 2.0.5. Only the first

steps of the pipeline were executed, i.e. the data were screened for pulse height (using limits 4–15) and corrected for Doppler effects of the satellite’s motion. Bursts were also removed, but no walk or drift correction was applied. Then the data were combined using the program `ttag_combine`. Nearby airglow lines were used to determine the constant height of the extraction window. The wavelength calibration was derived from the position of the airglow lines. The resulting spectra for sight line SL5 are shown in Figure 1. Lines of O VI  $\lambda\lambda 1032, 1038$  and C II\*  $\lambda 1037$  are clearly seen in the SL5 data. Due to the lower signal-to-noise ratio in the SL6 spectra, we will focus on the SL5 measurements in our analysis and refer only briefly to the SL6 data in section 3.

We followed the arguments of Shelton et al. (2001) to exclude terrestrial airglow, solar O VI emission, and scattered light inside the satellite as other possible explanations for the observed emission lines. Possible contamination ( $1\sigma$  upper limit) of O VI  $\lambda 1032$  by fluorescing H<sub>2</sub> is less than 200 LU (LU = photons s<sup>-1</sup> cm<sup>-2</sup> sr<sup>-1</sup>) for SL5. An unknown feature appears in the day-plus-night spectra on the blue side of O VI  $\lambda 1032$  but is absent in the night-only data. This feature is assumed to be airglow and has been seen in other data sets (e.g., Shelton et al. 2001). Due to its proximity to the O VI  $\lambda 1032$  line, reliable measurements for O VI could be obtained only from orbital night-time data.

### 3. RESULTS

We measured the line fluxes for SL5 in two ways. In the photon-counting method, we summed the counts in the wavelength region occupied by the emission line and subtracted a constant continuum derived from the surrounding spectrum. One-sigma uncertainties were derived assuming Gaussian statistics. In the second method, we used a line fitting algorithm, which determined the minimum  $\chi^2$  for a range of synthetic line profiles using three free parameters for each line: central wavelength, line width (FWHM), and peak intensity. The background was fitted by a straight line. We assumed that the emission line profiles were a convolution of a Gaussian with the instrumental line spread function, which for filled LWRS slit emission is a 106 km s<sup>-1</sup> wide flat-top profile. One-sigma uncertainties for each parameter were derived by varying the parameter and optimizing  $\chi^2$  with the other parameters until the newly calculated  $\chi^2$  had increased by 1 relative to the optimal solution (Avni 1976).

The results of both methods are given in Table 2 for the SL5 data.  $I_{\text{tot}}$  is the integrated intensity of the emission line, FWHM is the intrinsic line width, and  $\lambda_{\text{cen}}$  is the central wavelength of the line. The derived velocity was converted to the local standard of rest ( $v_{\text{LSR}}$ ). The large uncertainties of  $I_{\text{tot}}$  for O VI  $\lambda 1038$  and C II\*  $\lambda 1037$  in the  $\chi^2$  method reflect the close proximity of these features: reducing the strength of one line was compensated by

increasing the strength of the other, allowing a larger parameter space with only slow changes in  $\chi^2$ . The extinction toward SL5 is approximately  $E_{B-V} = 0.024$  (Schlegel, Finkbeiner, & Davis 1998), corresponding to an attenuation in the O VI intensity of  $\sim 30\%$ , if all of the reddening occurs in front of the O VI emitting gas and the extinction parameterization of Cardelli, Clayton, & Mathis (1989) is assumed. The line ratio O VI  $\lambda 1032$ /O VI  $\lambda 1038$  would approach 2 in optically thin gas, whereas in an optically thick medium the line ratio would approach 1 due to self-absorption. We derived a line ratio of  $2.0 \pm 0.8$ ; the large uncertainty makes it impossible to constrain the optical depth of the O VI emitting gas.

Our second sight line, SL6, lies near SL5 and shows O VI  $\lambda 1032$  emission in the day-plus-night spectrum. However, the emission line is only marginally detected in the night-only data and does not allow reliable measurements. The day-plus-night spectrum suggests an O VI  $\lambda 1032$  intensity and velocity comparable to those measured in the SL5 data.

#### 4. DISCUSSION

Figure 2 shows a schematic picture of the Milky Way. The positions of the four major spiral arms are adopted from Taylor & Cordes (1993). The model of HVC Complex C is based on H I contours (Wakker 2001) assuming a roughly constant thickness and  $z$  height for Complex C. No assumptions for the depth of Complex C are made. All O VI emission sight lines observed with *FUSE* are shown. While the other sight lines have Galactic latitudes of about  $60^\circ$  or more (except for sight line 2, hereafter SL2), SL5 has a latitude of only about  $40^\circ$ , thus probing a different part of the Milky Way.

SL5 intersects HVC Complex C at its southern boundary. Due to the large extinction of Complex C, it is unlikely that the observed O VI emission originates in gas beyond these HVCs, i.e. the location of Complex C can be considered an upper limit on the distance to the O VI emitting gas. A (weak) lower limit on the distance to Complex C at  $l \approx 90^\circ$  is 6 kpc (Wakker 2001). If the source of the O VI emission were the surface of infalling clouds, we could expect O VI emission at the same high velocities as measured in the Leiden-Dwingeloo H I Survey in this direction. The H I HVC component is observed at  $v_{\text{LSR}} = -115 \text{ km s}^{-1}$  (B. Wakker 2002, private communication). The SL5 data show no O VI counterpart at this velocity. The  $1\sigma$  upper limit for HVC O VI is 300 LU. We conclude that the observed O VI emission does not come from infalling HVCs.

The SL5 sight line passes  $\sim 3$  kpc above the Perseus arm (Fig. 2). The velocity of the Perseus arm in the direction of SL5 ( $l = 95^\circ.4$ ) is  $-70 \pm 10 \text{ km s}^{-1}$  (Kepner 1970). Assuming corotation of associated gas at higher altitudes, the Perseus arm velocity projected onto

sight line SL5 at  $b = 36^\circ.1$  is  $-58 \pm 8 \text{ km s}^{-1}$ . This is consistent with the velocities observed in the SL5 spectrum and implies that the O VI emitting gas has no velocity component perpendicular to the disk. Figure 3 shows a map of H $\alpha$  emission from the Wisconsin H-Alpha Mapper (WHAM) Survey (courtesy of M. Haffner & G. Madsen). A group of strong H $\alpha$  filaments extends between  $l = 85^\circ$  and  $110^\circ$  from the disk into the halo indicating an outflow of gas. Sight line SL5 intersects an H $\alpha$  filament above this region of strongest H $\alpha$  emission. The WHAM spectra closest to our SL5 pointing show H $\alpha$  emission at velocities ranging from  $-50$  to  $+20 \text{ km s}^{-1}$  (M. Haffner 2002, private communication). The H $\alpha$  filaments are most pronounced in the velocity range from  $-45$  to  $-25 \text{ km s}^{-1}$  at higher latitudes and  $-25$  to  $0 \text{ km s}^{-1}$  closer to the disk. This suggests that the outflow velocity decreases with  $z$  in H $\alpha$ . A simple Galactic rotation model (a corotating halo with  $v = 220 \text{ km s}^{-1}$ ) places gas with the observed O VI velocity at  $z \approx 5.5 \text{ kpc}$  and at a distance of  $\sim 9.3 \text{ kpc}$  from the Sun along sight line SL5 in the neighborhood of the Perseus arm H $\alpha$  filaments. The similar velocities of these filaments, the Perseus arm, and the O VI emitting gas suggest that these three components are associated with each other: The shock-heated gas ejected by supernova explosions in the Perseus arm and observed in SXR emission (Snowden et al. 1997) is cooling down or mixing with cooler gas and emitting the O VI photons that we see. The O VI emitting gas is on the verge of falling back to the disk, while the underlying outflow supplies new, hot gas.

The measured intensities in the SL5 data ( $1600 \pm 300 \text{ LU}$  at  $1032 \text{ \AA}$  and  $800 \pm 300 \text{ LU}$  at  $1038 \text{ \AA}$ ) are lower than all previously measured O VI emission line intensities ( $2000$ – $3300$  and  $1100$ – $2000 \text{ LU}$ , respectively). All the previous sight lines point toward high Galactic latitudes inside what Welsh et al. (2002) call the Local Interstellar Chimney. Only SL2 and SL5 (both at  $|b| \approx 40^\circ$ ) appear to intersect the walls of the Local Bubble and the Chimney (see Sfeir et al. 1999 for contours). A new study by Shelton (2002b) yields  $2\sigma$  upper limits of  $420 \text{ LU}$  ( $1032 \text{ \AA}$ ) and  $540 \text{ LU}$  ( $1038 \text{ \AA}$ ) for O VI emission originating in the Local Bubble, intensities much lower than any of the O VI detections. This suggests that a significant fraction of the observed O VI emission along SL2 and SL5 originates beyond the Local Bubble. The lower intensities in the SL5 data can be explained by more extinction due to the larger distance to the O VI emitting region, if it in fact lies above the Perseus arm as suggested above. Although the O VI intensities differ by a factor of about 2 between SL2 and SL5, the SXR fluxes are similar ( $930 \pm 60$  and  $944 \pm 15 \times 10^{-6} \text{ counts s}^{-1} \text{ arcmin}^{-2}$ , respectively; Snowden et al. 1997<sup>1</sup>). It is not clear whether most of the observed SXR emission comes from the same region as the O VI emission.

The correlations among the velocities of spiral arms, H $\alpha$  filaments, and O VI emitting

---

<sup>1</sup>Values obtained using the NASA HEASARC X-Ray Background Tool at <http://heasarc.gsfc.nasa.gov/cgi-bin/Tools/xraybg/xraybg.pl>

gas that we find for SL5 are not present for any of the previously-observed O VI emission sight lines. For example, the spiral arm and O VI velocities along SL2 are consistent only if the O VI emitting gas has an outflow velocity of  $100 - 170 \text{ km s}^{-1}$  at  $z = 1 - 9 \text{ kpc}$ . No  $\text{H}\alpha$  filaments or other signs of outflows were found near the previously-observed sight lines. (Note: SL2 points toward a region not observed by the WHAM survey.) The corotating halo model would place the O VI emitting gas  $10 - 20 \text{ kpc}$  above the plane (sight lines 2, 4a, 4b) or even higher ( $> 600 \text{ kpc}$  and  $> 70 \text{ kpc}$  for sight lines 1a and 1b); sight line 3 yields positive O VI velocities, whereas the model requires negative velocities. We therefore conclude that SL5 is the only sight line for which a reasonable and consistent explanation of the O VI emission and its parameters can be found, and that SL5 and possibly SL6 probe halo gas that originated in the underlying spiral arm.

## 5. CONCLUSIONS

We have observed Galactic O VI emission along two low-latitude sight lines, only one of which yields reliable measurements. Based on the observed velocities of the O VI emitting gas, the  $\text{H}\alpha$  filaments, and the underlying spiral arm, we conclude that the O VI emission seen along sight line SL5 (and probably SL6) originates in the halo about  $\sim 3 \text{ kpc}$  above the Perseus arm. Our observations are consistent with a Galactic fountain scenario in which gas is heated and ejected by supernova explosions in the spiral arms, becomes boyant in the colder disk gas, and rises into the halo where it cools down and sooner or later falls back to the disk. We find no O VI counterpart to the HVC component observed in H I.

This research is supported by NASA contract NAS5-32985 to the Johns Hopkins University. The authors thank L. M. Haffner and G. J. Madsen for creating the WHAM map. The Wisconsin H-Alpha Mapper is funded by the National Science Foundation. The authors are also thankful to B. P. Wakker for his comments on HVC Complex C and the H I line profiles. This work made use of the NASA Extragalactic Database (NED) and the NASA Astrophysics Data System (ADS).

## REFERENCES

- Ake, T. B., Class, B. F., Roberts, B. A., Kruk, J. W., Blair, W. P., Moos, H. W., & *FUSE* Operations Team 2002, BAAS, 34, 671
- Avni, Y. 1976, ApJ, 210, 642
- Cardelli, J. A., Clayton, G. C., & Mathis, J. S. 1989, ApJ, 345, 245
- Dixon, W. V., Sallmen, S., Hurwitz, M., & Lieu, R. 2001, ApJ, 552, L69
- Kepner, M. 1970, A&A, 5, 444
- Martin, C., & Bowyer, S. 1990, ApJ, 350, 242
- Moos, H. W., et al. 2000, ApJ, 538, L1
- Sahnow, D. J., et al. 2000, ApJ, 538, L7
- Savage, B. D., et al. 2002, ApJS, in press
- Schlegel, D. J., Finkbeiner, D. P., & Davis, M. 1998, ApJ, 500, 525
- Sfeir, D. M., Lallement, R., Crifo, F., & Welsh, B. Y., 1999, A&A, 346, 785
- Snowden, S. L., et al. 1997, ApJ, 485, 125
- Shelton, R. L. 2002a, ApJ, 569, 758
- Shelton, R. L. 2002b, BAAS, 34, 1310
- Shelton, R. L., et al. 2001, ApJ, 560, 730
- Taylor, J. H., & Cordes, J. M. 1993, ApJ, 411, 674
- Wakker, B. P. 2001, ApJS, 136, 463
- Welsh, B. Y., Sallmen, S., Sfeir, D., Shelton, R. L., & Lallement, R. 2002, A&A, 394, 691

Table 1. OBSERVATIONS

Position	Program ID	$\alpha$ (h m s) <sup>a</sup>	$\delta$ (d m s) <sup>a</sup>	$l$ (deg) <sup>a</sup>	$b$ (deg) <sup>a</sup>	Exposure Time (s) <sup>b</sup>
SL5	S4054801	16 59 38.39	65 00 43.83	95.4	36.1	217352/94829
SL6	S4056101	15 46 02.23	65 01 37.87	99.3	43.3	31553/13114

<sup>a</sup>Coordinates are J2000

<sup>b</sup>Day-plus-night/night only

Table 2. EMISSION LINE PARAMETERS FOR SL5

Line	$I_{\text{tot}}^{\text{ab}}$ (ph s <sup>-1</sup> cm <sup>-2</sup> sr <sup>-1</sup> )	$I_{\text{tot}}^{\text{bc}}$ (ph s <sup>-1</sup> cm <sup>-2</sup> sr <sup>-1</sup> )	FWHM <sup>b</sup> (km s <sup>-1</sup> )	$\lambda_{\text{cen}}$ (Å)	$v_{\text{LSR}}$ (km s <sup>-1</sup> )
O VI $\lambda$ 1031.926	1600 ± 300	1680 ± 90	75 ± 3	1031.7 ± 0.1	-50 ± 30
O VI $\lambda$ 1037.617	800 ± 300	900 ± 700	22 ± 15	1037.40 ± 0.02	-44 ± 6
C II* $\lambda$ 1037.02	1000 ± 300	1300 ± 900	40 ± 20	1036.77 ± 0.04	-53 ± 12

<sup>a</sup>Integrated intensity using photon-counting method

<sup>b</sup>Systematic uncertainties are not included in error estimates.

<sup>c</sup>Integrated intensity using minimum  $\chi^2$  method

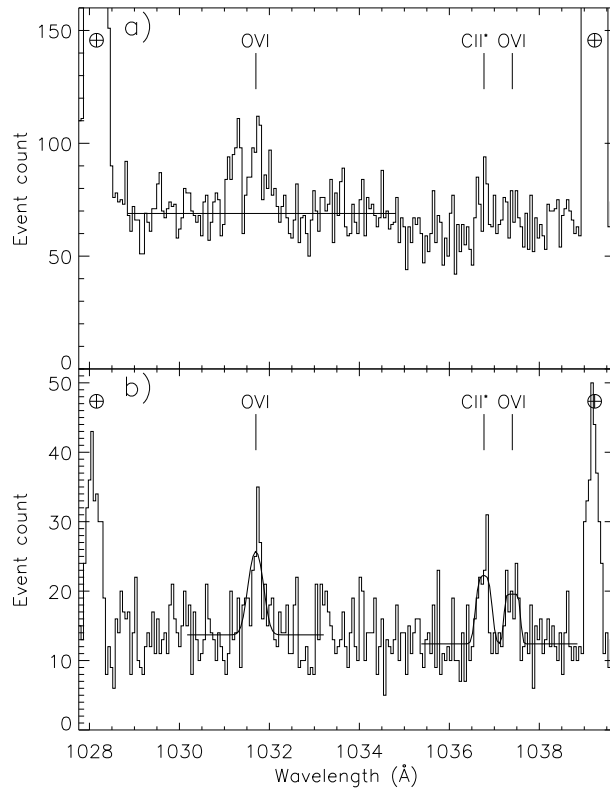


Fig. 1.— The SL5 spectra around the O VI doublet. Both day-plus-night (a) and night only spectra (b) are shown. Both spectra were binned by 8 pixels for display only. Panel a shows the continuum fit for O VI  $\lambda$ 1032; panel b shows the minimum  $\chi^2$  fits for the emission lines in SL5. The fitted positions of the O VI doublet and the C II\* line are labeled. Airglow lines are marked with the Earth symbol.

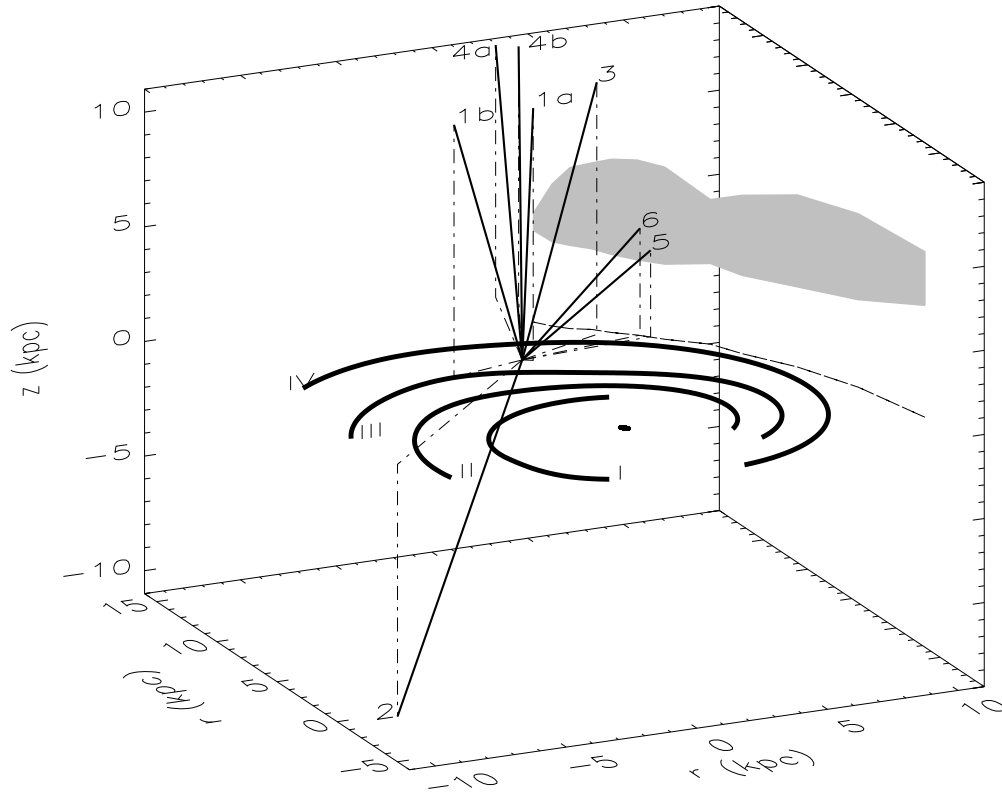


Fig. 2.— 3D model of the Milky Way. The four major spiral arms are shown as thick lines in the  $z = 0$  plane: I = Norma, II = Scutum-Crux, III = Sagittarius-Carina, IV = Perseus. The light grey area represents a model for HVC Complex C. The projection of Complex C into the Galactic disk is shown as a dashed line. The O VI emission sight lines are shown as solid, straight lines with their projections into the disk shown as dash-dotted lines: 1a, b = Dixon et al. (2001); 2 = Shelton et al. (2001); 3 = Shelton (2002a); 4a, b = Welsh et al. (2002); 5 = SL5; 6 = SL6. All sight lines are cut off at  $|z| = 11$  kpc, except sight lines 5 and 6, the only sight lines intersecting HVC Complex C and thus cut off at the Complex C surface.

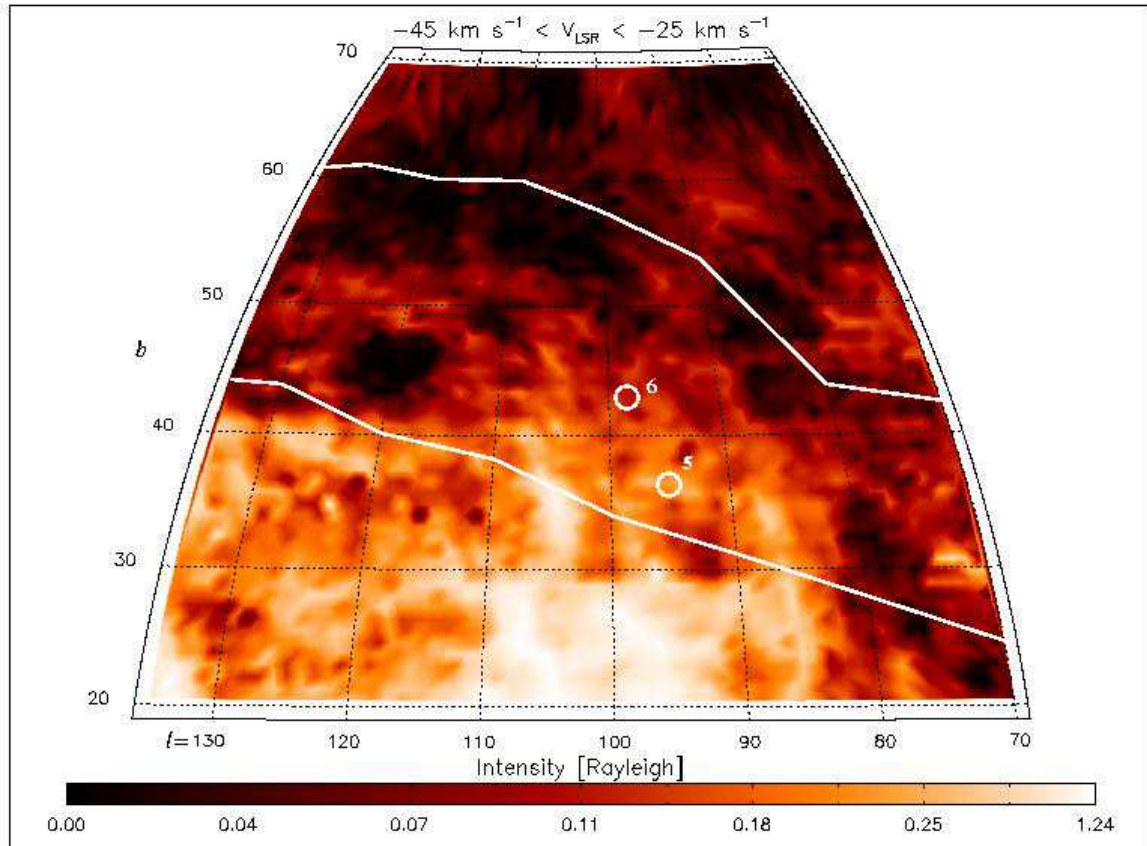


Fig. 3.—  $\text{H}\alpha$  image with *FUSE* positions and HVC Complex C boundaries marked. The  $\text{H}\alpha$  emission is integrated over the velocity range from  $-45$  to  $-25 \text{ km s}^{-1}$ ; the intensity scale is not linear (courtesy of M. Haffner & G. Madsen). Overlaid in white are the faintest contours of HVC Complex C (Wakker 2001). The positions of the SL5 and SL6 *FUSE* sight lines are marked as circles. Note that the circles are not scaled to the size of the LWRS aperture. The brightest  $\text{H}\alpha$  emission at the bottom of this map ( $l = 85^\circ - 110^\circ$ ) is part of a group of strong filaments extending from the disk into the halo.